Drug screening approach against mycobacterial fatty acyl-AMP ligase FAAL32 renews the interest of the salicylanilide pharmacophore in the fight against tuberculosis

Nguyen-Hung Le, Patricia Constant, Samuel Tranier, Virginie Nahoum, Valérie Guillet, Laurent Maveyraud, Mamadou Daffé, Lionel Mourey, Pierre Verhaeghe, Hedia Marrakchi

▶ **To cite this version:**

Nguyen-Hung Le, Patricia Constant, Samuel Tranier, Virginie Nahoum, Valérie Guillet, et al.. Drug screening approach against mycobacterial fatty acyl-AMP ligase FAAL32 renews the interest of the salicylanilide pharmacophore in the fight against tuberculosis. Bioorganic and Medicinal Chemistry Letters, 2022, 71, pp.116938. 10.1016/j.bmc.2022.116938 . hal-03758907

HAL Id: hal-03758907
https://hal.science/hal-03758907v1

Submitted on 18 Oct 2022

HAL is a multi-disciplinary open access archive for the deposit and dissemination of scientific research documents, whether they are published or not. The documents may come from teaching and research institutions in France or abroad, or from public or private research centers.

L'archive ouverte pluridisciplinaire **HAL**, est destinée au dépôt et à la diffusion de documents scientifiques de niveau recherche, publiés ou non, émanant des établissements d'enseignement et de recherche français ou étrangers, des laboratoires publics ou privés.

Drug screening approach against mycobacterial fatty acyl-AMP ligase FAAL32 renews the interest of the salicylanilide pharmacophore in the fight against tuberculosis

Nguyen-Hung Le[1†], Patricia Constant[1], Samuel Tranier[1], Virginie Nahoum[1], Valérie Guillet[1], Laurent Maveyraud[1], Mamadou Daffé[1], Lionel Mourey[1*], Pierre Verhaeghe[2,3*] and Hedia Marrakchi[1*]

From the [1]Institut de Pharmacologie et de Biologie Structurale, IPBS, Université de Toulouse, CNRS, UPS, Toulouse, France; [2]Laboratoire de Chimie de Coordination (LCC), Université de Toulouse, CNRS, UPS, Toulouse, France; [3]CHU de Nîmes, Service de Pharmacie, Nîmes, France.

† Present address: Aix-Marseille Université - CNRS UMR 7283, Institut de Microbiologie de la Méditerranée and Turing Center for Living Systems, Marseille, France

KEYWORDS: *Mycobacterium tuberculosis*; fatty acyl-AMP ligase; FAAL32; salicylanilides; antimycobacterials; drug screening

ABSTRACT

Tuberculosis (TB) remains a global health crisis, further exacerbated by the slow pace of new treatment options, and the emergence of extreme and total drug resistance to existing drugs. The challenge to developing new antibacterial compounds with activity against *Mycobacterium tuberculosis* (Mtb), the causative agent of TB, is in part due to unique features of this pathogen, especially the composition and structure of its complex cell envelope. Therefore, targeting enzymes involved in cell envelope synthesis has been of major interest for anti-TB drug discovery. FAAL32 is a fatty acyl-AMP ligase involved in the biosynthesis of the cell wall mycolic acids, and a potential target for drug discovery. To rapidly advance research in this area, we initiated a drug repurposing campaign and screened a collection of 1280 approved human or veterinary drugs (Prestwick Chemical Library) using a biochemical assay that reads out FAAL32 inhibition. These efforts led to the discovery of salicylanilide closantel, and some of its derivatives as inhibitors with potent *in vitro* activity against *M. tuberculosis.* These results suggest that salicylanilide represents a potentially promising pharmacophore for the conception of novel anti-tubercular candidates targeting FAAL32 that would open new targeting opportunities. Moreover, this work illustrates the value of drug repurposing campaigns to discover new leads in challenging drug discovery fields.

Introduction

Despite the availability of a vaccine and several antibiotics, tuberculosis (TB) remains the deadliest disease due to a single infectious agent, *Mycobacterium tuberculosis* (Mtb) (except for the year 2020 where TB was surpassed by COVID-19), and claims about 1.4 million lives each year (*1*). The expansion of drug resistance has added an alarming dimension to this global health crisis, with the emergence of extremely- (XDR) and totally-drug-resistant (TDR) strains. This underscores the urgent need to develop antimycobacterial agents with novel mechanisms of action (MOA) (*2*).

A unique feature of mycobacteria is their complex cell envelope, which is rich in diverse essential and/or virulence-conferring lipids (*3*, *4*), including mycolic acids (MAs). Notably, the first-line anti-TB drug isoniazid (INH) and the recently-approved delamanid, efficient against MDR-TB, target the MA synthesis. MAs are exceptionally long (C_{70}-C_{90}), alpha-branched, beta-hydroxylated fatty acids, and essential for the survival and virulence of Mtb. Therefore, targeting such crucial lipid biosynthetic pathways could afford new classes of anti-tubercular agents. The MAs biosynthesis relies on the action of fatty acyl-AMP ligases (FAALs), a class of functionally non-redundant fatty acid adenylating enzymes that serve to link fatty acid and polyketide (PKS) synthesis in mycobacteria. FAAL32 (also known as FadD32) is required for the activation as acyl-AMP of the very long meromycolic chain of MAs (*3*, *5*). Following acyl activation, FAAL32 transfers long acyl chains onto the condensase Pks13, to perform the condensation with a C_{24}-C_{26} fatty acid to yield the direct precursor of MAs (*6–10*) (Fig. 1). The operon *faal32-pks13-accD4* is highly conserved in all mycobacterial species and essential for the viability of mycobacteria (*11*). Conditional expression of *faal32* confirmed its essentiality for the growth of Mtb while knockdown studies have established that the *faal32* operon is a vulnerable target (*10*, *12*). Therefore, FAAL32 may represent a potentially promising anti-TB target.

Since FadD is a newly discovered family of adenylate-forming enzymes in Mtb, there are very few reported inhibitors, belonging to two distinct chemical families (Fig. 1). First, coumarin derivative CCA34 and its quinoline structural analogue inhibit FAAL32 by blocking the protein's acyl transferase activity onto Pks13 (*13*, *14*). Second, the AMP analogues AMPC12 and the nonhydrolyzable alkanoyl adenosine monosulfamate AMS inhibit the acyl-AMP ligase activity (*6*–*8*). Adenosine 5′-alkyl phosphates (including 5′-dodecylphosphate, AMPC12) are structural analogues of adenosine 5′-acyl phosphates (acyl-AMP), the transient intermediates of the acyl-CoA/ACP synthetic reaction and were used to solve the 3D structure of FAAL32 (6, 7). Moreover, a recent study highlighted spirothiazolidinones as new antimycobacterial derivatives that could target FAAL32 (*15*) while a very recent *in silico* study revealed that the drugs mefloquine, sorafenib and loperamide appear as good candidates for inhibiting Mtb FAAL32 (*16*).

We previously developed an enzymatic assay for FAAL32 that was adapted to high throughput screening (HTS) format (*17*). Herein, we describe the optimization and automatization of this biochemical assay to search for new FAAL32 inhibitors by screening the Prestwick Chemical library of 1280 approved (veterinary or human) drugs. Hit selection and further validation in Mtb viability assays identified the salicylanilide pharmacophore as a new previously-unknown chemotype targeting this essential enzyme and displaying a potent anti-Mtb activity.

Material and methods

Spectrophotometric enzyme assays. All assays were performed in 384-well polystyrene microplates (Greiner BioOne, Courtaboeuf, France), using the Pi ColorLock™ Gold kit (Innova Biosciences, Cambridge, UK) as described (*17*). Briefly, 1 µL of compound or DMSO was added to each well containing 15 µL of substrate mix (50 mM HEPES pH 7.5, 8 mM $MgCl_2$, 0.01% Brij®58, 2 mM ATP, 20 µM lauric acid, 1 mM DTT and 2 mU/mL pyrophosphatase (Sigma Aldrich, USA)).

Reactions were initiated by addition of 14 µL of purified Mtb FAAL32 protein at 400 nM final concentration (*18*). After 50 min of incubation at 37 °C, reactions were stopped by adding 10 µL of Goldmix, followed by 5 µL of Stabilizer and 35 µL of 50 mM HEPES buffer. The A_{630} was read after 15 min incubation at RT in a ClarioStar plate reader (BMG Labtech, Germany). To calculate the concentration of Pi released corresponding to half concentration of FAAL32 product, a calibration curve using known concentrations of Pi varying from 10 µM to 80 µM was performed in each experiment according to the manufacturer's recommendations.

For inhibition studies using the bi-substrate analog dodecyl-adenosine monophosphate AMPC12, concentrations of ATP and lauric acid were adjusted to be above or around the K_m (0.25 mM ATP and 20 µM lauric acid). The AMPC12, chemically synthesized as described previously (*8*), was first diluted in DMSO and applied at increasing concentrations to the substrate mixture. The reaction was started by adding the enzyme. Data were expressed as percentage of inhibition. Curve fitting and IC_{50} calculations were performed using sigmoidal dose response as equation model (GraphPad Prism 5.04 Software, San Diego, CA).

Automatic screening method validation. In order to validate the automatic pipetting accuracy, a stock solution of Ponceau S (Ponceau red) was prepared at 2.5 mg/mL in pure DMSO. For standard values, 1 to 4 µL of stock solution were diluted into 80 µL total volume of water in a 384-well microplate and absorbance was read at 560 nm using a ClarioStar plate reader (BMG Labtech, Germany). The same dilutions were prepared either manually or using the 96-multichannel head of a Biomek FX^P liquid handler (Beckman Coulter). 100 µL of Ponceau S stock solution were distributed evenly in a round bottom 96-wells microplate.

The following protocol was used for activity and inhibition assays as well as negative and positive controls. 1 µL was pipetted into 384-well destination plate from either a source plate containing

stock solutions of EDTA 0.5 M (positive inhibition control), $MnCl_2$ 0.66 M (alternative positive inhibition control), DMSO (Blank) or increasing concentrations of AMPC12 (0.1 to 31.6 µM). Next, 15 µL of 2X substrate mix (100 mM Hepes buffer pH 7.5, 16 mM $MgCl_2$, Brij35 0,002%, 150 µM lauric acid, 2 mM ATP, 2 mM DTT and 0,02 U/mL pyrophosphatase) and 14 µL of protein solution at 856 nM concentration were sequentially pipetted into the destination plate. After 50 min incubation at 30 °C, 10 µL of Goldmix, 5 µL of stabilizer and 20 µL of 50 mM Hepes pH 7.5 were added and the absorbance was immediately read at 630 nm.

Search for FAAL32 activity inhibitors by screening. The Prestwick Chemical Library containing 1280 molecules was distributed into four 384-well plates, each containing 320 compounds at 1 mM concentration. 1 µL of each compound was pipetted into the destination plate. The rest of the screening sequence was as described above. For each plate, columns 1 and 2 were dedicated to the positive inhibition control in presence of 0.5 M EDTA solution while columns 23 and 24 were dedicated to the negative inhibition control in presence of DMSO.

IC_{50} Determination. For inhibition studies, the substrate analogue alkyl-adenylate AMPC12 (chemically synthesized as described previously (*8*) or selected compounds were first diluted in DMSO to a series of final concentrations ranging from 0.5 to 66 µM. Next, 1 µL of each molecule was added to the substrate mixture. The reaction was started by enzyme addition and A_{630} was measured and expressed as a percentage of inhibition. Curve fitting and IC_{50} calculations were performed using sigmoidal dose response as equation model (GraphPad Prism 5.04 Software, San Diego, CA).

Thermal unfolding analysis using nanoDSF. For melting temperature measurements, FAAL32 was mixed with different amounts of closantel or rafoxanide (0.5 µM FAAL32 and 0.5-10 µM for ligand) in 50 mM HEPES, pH7.5, 500 mM NaCl, 5% DMSO. The samples were incubated at room

temperature for 5 min and then loaded into high-sensitivity capillaries filled with 10 µl of sample; excitation light was set on autodetect, and samples were measured in temperature range of 20 to70 °C with a temperature slope of 1 °C/min, using the Prometheus Panta (NanoTemper Technologies GmbH, Munich, Germany). For determination of the protein melting point (T_m), the ratio of the fluorescence intensities at 330 and 350 nm (F350/F330) was plotted, reflecting local chemical environment changes of tryptophan and tyrosine residues. Thermal unfolding and aggregation curves were read using the Panta analysis software (NanoTemper Technologies GmbH, Munich, Germany) and derivatives of experimental curves were computed to facilitate visualization.

Mtb growth inhibition assay. Colorimetric microassay based on the reduction of tetrazolium salts (MTT) was used to measure the susceptibility of Mtb to test molecules by determining their minimum inhibitory concentration (MIC) (*19*). Cells growing as surface pellicle were recovered from 100 mL culture in 7H9 broth medium containing 0.2% glycerol, vortexed with 4 mm glass beads and suspended with 20 mL 7H9/0.2% glycerol broth. The suspension was then centrifuged at 800 rpm to eliminate residual bacterial clumps. The supernatant was used to prepare mycobacterial suspension at A_{600} of 0.1. 2 µL of selected compounds at 1 mM in DMSO or of serial 2-fold dilutions prepared in DMSO when mentioned were added in wells of a 96-well flat bottom microplate (Nunc) containing 100 µL of 7H9/0.2% glycerol broth. For no inhibition control wells, 2 µL of DMSO were added instead. 100 µL of mycobacterial suspension were then added. The microplates were incubated for 6 d at 37 °C and 50 µL of freshly prepared solution of Thiazolyl Blue Tetrazolium Bromide (Sigma, 1 mg/mL in 7H9 medium) were added to each well. Plates were incubated for a further 24 h. In living bacteria, tetrazolium salts were reduced to insoluble formazan which were solubilized by adding 50 µL of SDS 20%. After 24 h, the microplates were read at 570 nm with a microplate reader Expert Plus (ASYS HITECH, Austria). MIC was determined as the

lowest concentration of drug that inhibited bacterial growth (absorbance value for untreated bacilli was taken as a growth control). IC_{50} was determined using GraphPad Prism 5.04 software.

Docking and molecular dynamics simulations. Docking of compounds was performed with AutoDock Vina (*20*), as previously described (*21*). Briefly, several conformations of FAAL32 were generated using molecular dynamics simulation starting from either the structure of FAAL32 in complex with 5'-O-[(11-phenoxyundecanoyl) sulfamoyl]adenosine (PDBID 5HM3, Kuhn et al. 2016), a model of apo FAAL32 extracted from 5HM3, or a model of FAAL32 in complex with AMPC12 (PDBID 5EY9, reference Guillet 2016). Most different conformations were extracted from the 110 ns simulation performed with Amber15 (*22*), resulting in 26 distinct conformations of FAAL32. All compounds tested were docked onto all conformations of FAAL32, and the 5 best poses, according to the Vina score, were used for the estimation of binding energy using the MM-PB/GBSA method, as available in the Amber suite. 120-ns simulations were performed for each of the selected poses and 1000 frames were extracted from the trajectory for binding energy computation with the MMPBSA.py.MPI script (*23*).

Results and Discussion

Assay automatization and validation. Assay automatization for the Mg^{2+}-ATP dependent fatty acyl-AMP ligase reaction (Fig. 1A) and accuracy of the method were implemented as described in Experimental Procedures (Fig. S1). We used DMSO as a positive control (FAAL32 full activity). For the negative control, addition of EDTA or $MnCl_2$ to the reaction mixture at a final concentration of 50 mM or 66 mM, respectively, was tested. Mn^{2+} mimics Mg^{2+} while EDTA is a chelating agent, both are frequently used to inhibit the Mg^{2+}-ATP complex formed during the adenylating reaction (17). Thus, EDTA was chosen as the negative control (100% inhibition) for the subsequent experiments based on its higher inhibitory effect on FAAL activity (Fig. S1).

To assess the reproducibility of the screening method and progress towards HTS, the Z'-factor of the automatic screening procedure was calculated using the chosen (negative and positive) controls as described (18). This yielded a value of 0.86, higher than the conventional 0.5 threshold set for a good HTS protocol (18), thus validating the reproducibility of the method (Fig. S1).

Finally, to validate the general performance of the automatic procedure for screening assays, we performed FAAL32 inhibition assays in the presence of the bi-substrate analogue AMPC12, previously shown to inhibit enzyme activity (6, 8, 15), either manually or using the liquid handling system. Comparison of both methods showed superimposable inhibition curves with half-inhibitory concentration (IC_{50}) values displaying minor and non-significant differences, i.e. 0.32 µM and 0.40 µM for manual control and semi-automatic assay, respectively (Fig. 1C). Altogether, these performance assays were conclusive for the use of the automatic assay for biochemical screening of FAAL32 activity.

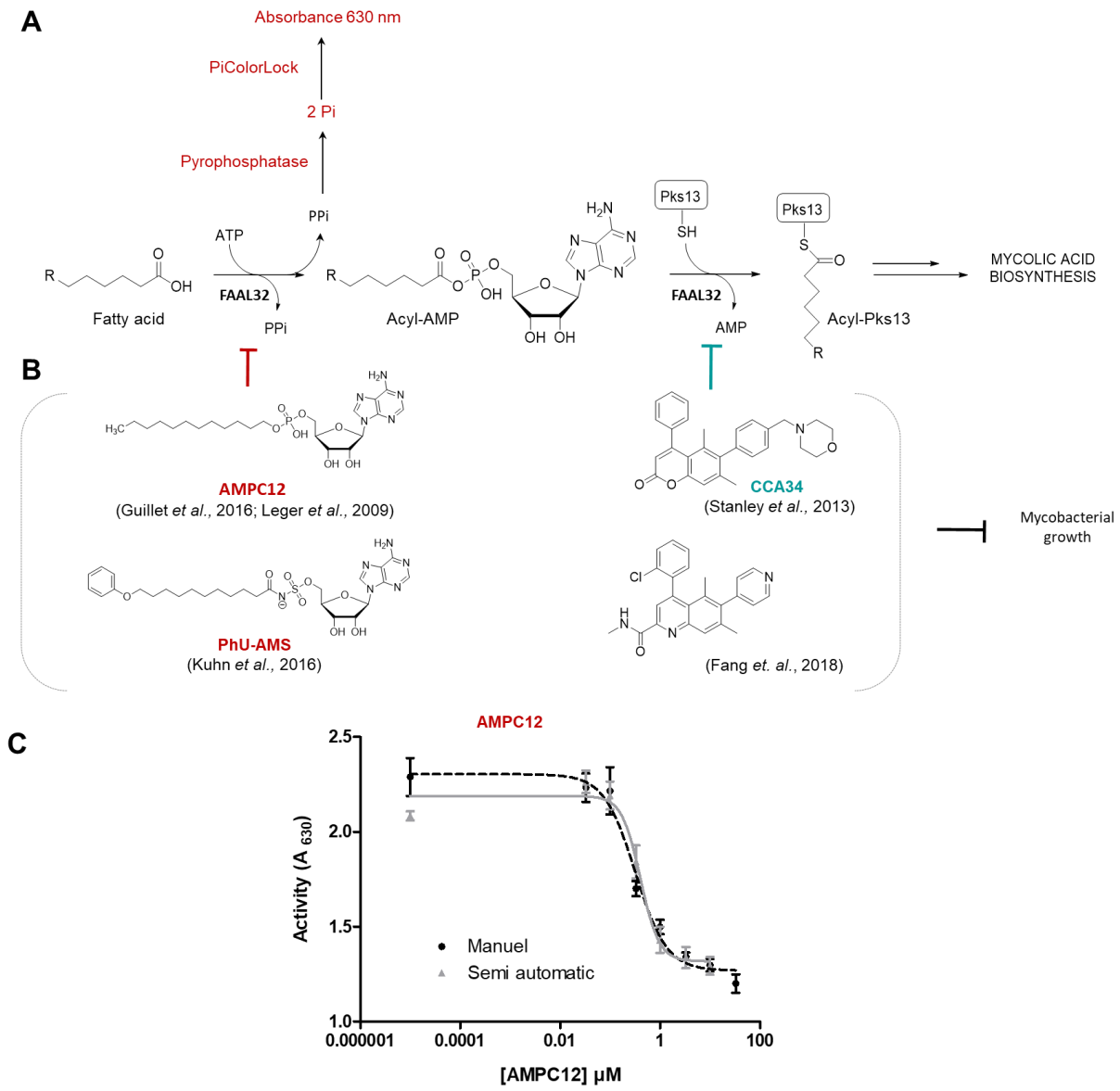

Fig. 1: FAAL32 two-step reaction mechanism, enzyme assay development and automation. A. Fatty acyl-AMP (FAAL) and Fatty acyl-ACP ligase half-reactions catalyzed by FAAL32 and coupled enzyme assay adapted for HTS (as described in ref 15). **B**. Known FAAL32 inhibitors of 1st and 2nd half reactions. **C**. Validation of general performance of robot for inhibition assays. Inhibition curves of FadD32 activity by substrate analog (alkyl C12-AMP) using either manual or semi-automatic method.

Chemical library screening for inhibitors of FAAL32 activity. We used our assay to screen the commercially available Prestwick Chemical Library® composed of 1280 off-patent small molecule drugs approved for human or veterinary use (Fig. 2A). In the primary screen, the biochemical assay

was performed in monoplicate at a compound concentration of 33 µM. The screen resulted in 36 hits (3% hit rate), defined as a compound that gave greater than 50% inhibition at 33 µM (Fig. 2A). For hit validation, the concentration response curves of these 36 molecules were analyzed manually in duplicate. 21 compounds displaying IC_{50} values below 100 µM were retained. These hit-compounds were mainly part of 6 therapeutic families: antiseptics & detergents (hexachlorophen, dequalinium, alexidine, merbromin and thonzonium), estrogens (hexestrol, dienestrol and diethylstilestrol), thyroid hormones (tiratricol, liothyronine and thyroxine), curares (alcuronium and cisatracurium), antiasthmatics (montelukast and pranlukast), and several antiparasitics including the salicylanilide derivative closantel (Table S1).

Hit evaluation and validation. To further evaluate the anti-Mtb activity of the hits inhibiting FAAL32 activity, 14 commercially available compounds among the 21 previously selected hits were tested for their capacity to inhibit Mtb H37Rv growth. Each compound was first evaluated at 10 µM in duplicate, using MTT colorimetric assay (*19*) in microplate with the first-line anti-TB drug INH as inhibition positive control (Fig. 2B). Among the 14 tested molecules, 11 showed at least 90% growth inhibition. Subsequently, we determined the minimum inhibitory concentration (MIC) for 8 compounds (Table S2). Out of these 8 compounds, thonzonium, alexidine, montelukast, merbromine, miconazole and verteporfin were not further studied because of their poor *in vitro* activity against Mtb (MIC > 1 µM), in comparison with INH. Moreover, several of these molecules are well known for their high toxicity (merbromin) or poor oral bioavailability (alexidine and thonzonium), making them unsuitable for pharmaceutical development. Despite promising *in vitro* antibacterial activity (MIC = 0.08 µM), hexachlorophene was also excluded because of its highly documented toxicity for human health. Thus, our study focused on closantel,

an anthelminthic veterinary drug. This compound was not only the most active inhibitor of FAAL32 identified in this screening (IC_{50} = 7.7 µM), but also the strongest *in vitro* anti-mycobacterial

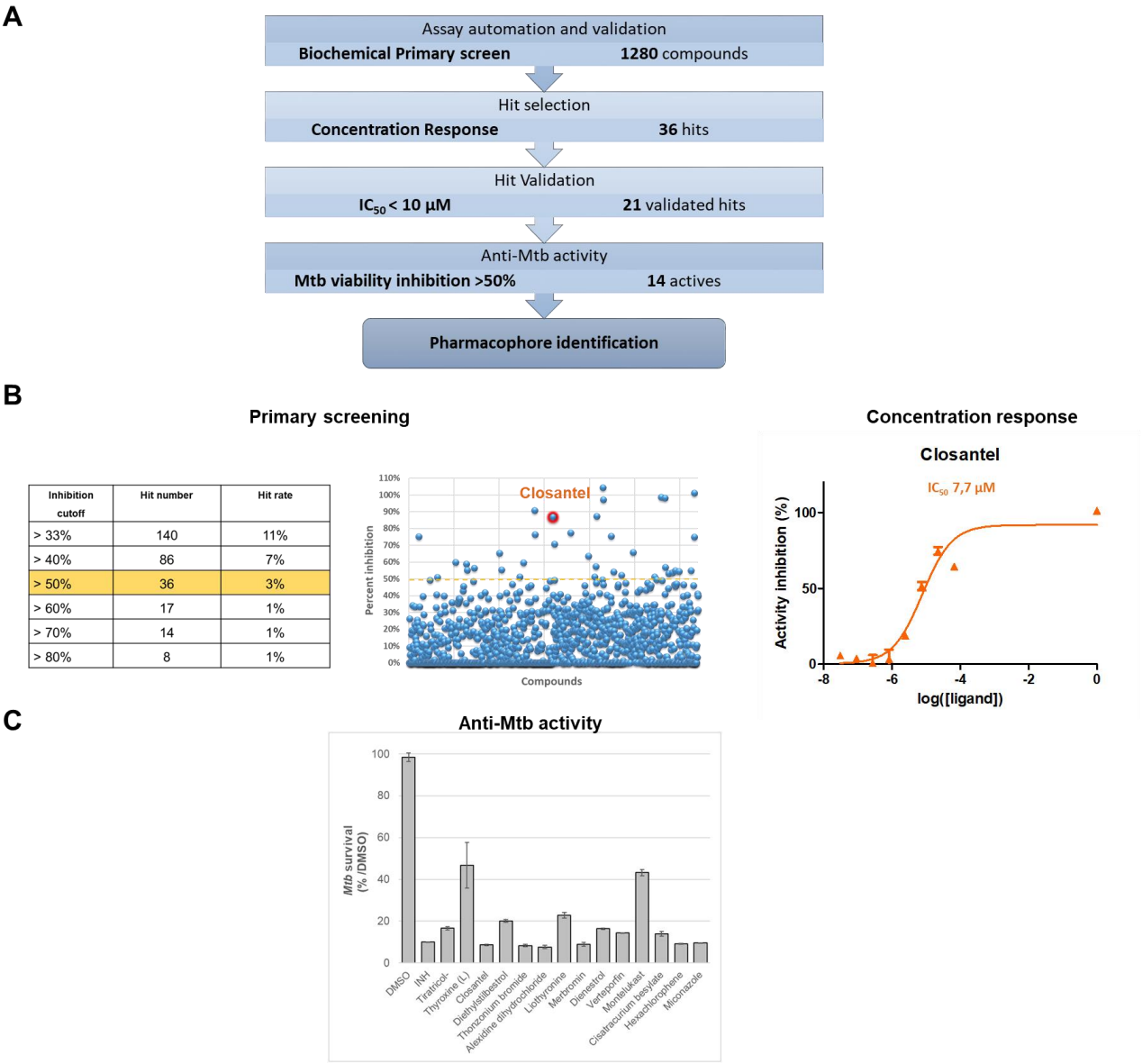

Inhibition cutoff	Hit number	Hit rate
> 33%	140	11%
> 40%	86	7%
> 50%	36	3%
> 60%	17	1%
> 70%	14	1%
> 80%	8	1%

Fig. 2: Screening the FAAL32 activity identifies hits active on Mtb growth. A. Workflow of the chemical library screening against FAAL32 activity and on *Mtb* viability *in vitro* . **B**. Primary screening of the chemical library at 33 µM and concentration response curve for the hit closantel. **C**. Hit activity on Mtb viability in monodose at 10 µM. The negative (DMSO) and positive (Isoniazid INH) controls of inhibition are indicated. *Mtb* survival is calculated relative to DMSO control.Tiratricol: Tiratricol,3,3',5-triiodothyroacetic acid.

molecule (MIC = 0.08 μM). Quite interestingly, this compound belongs to the salicylanilide family that was previously reported to display *in vitro* anti-mycobacterial activity (MIC in the μM range; Fig. S1) (*24–28*). However, although these compounds were proposed to act by disrupting the proton gradient *via* proton shuttling (*29*) or by inhibiting Mtb isocitrate lyase and methionine aminopeptidase (*30*), their exact mechanism of action has remained incompletely characterized.

Therefore, to examine whether salicylanilides inhibit Mtb growth, we obtained four commercially available compounds from this drug family (niclosamide, rafoxanide, oxyclosanide, and nitaxozanide; Fig. 3A) for further testing. All four compounds inhibited Mtb growth, with MIC below 0.4 μM (Fig. 3B), with the exception of the thiazole-containing derivative nitazoxanide (MIC 10 μM). Our results, taken together with previously reported low toxicity effects on mammalian cell viability for closantel, rafoxanide, and oxyclozanide (*31*), suggest that the salicylanilide pharmacophore may represent a promising starting point for developing FAAL32-directed inhibitors as a new class of Mtb drugs. However, closantel itself cannot be developed as an antitubercular candidate because of toxicity issues in Human, due to oxidative phosphorylation disruption causing optic nerve damage (*32*).

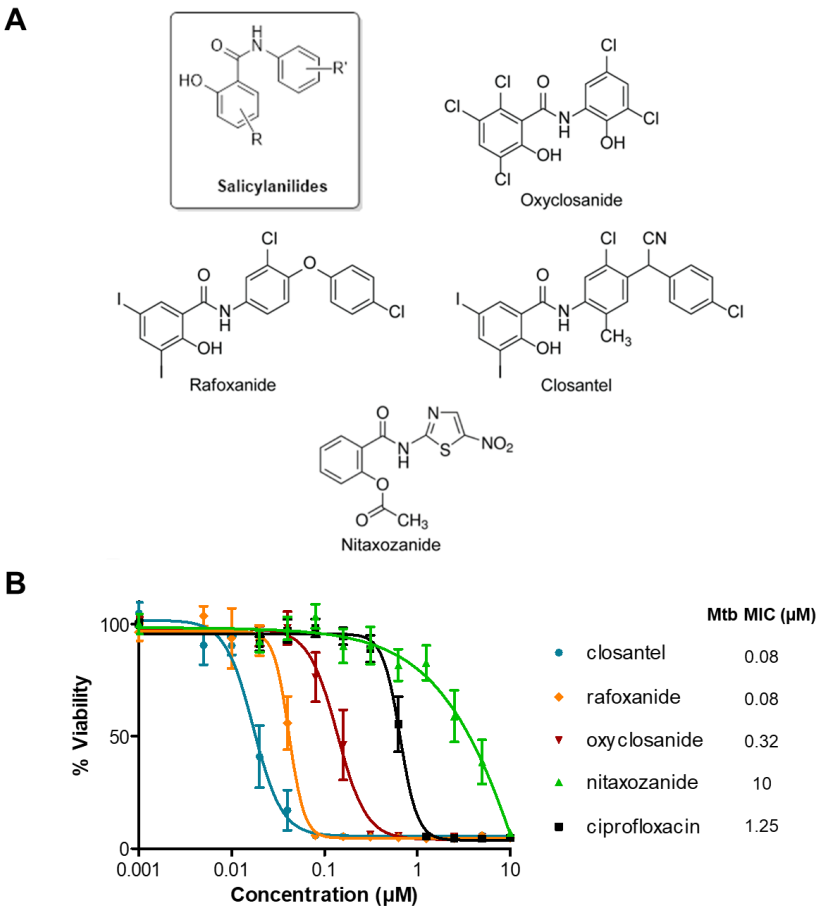

Fig. 3: Dose response Effect of salicylanilide-type FAAL32 inhibitors on *Mtb* viability. A. Selected representatives of the salicylanilide scaffold. **B.** Confirmation of hits (concentration-response analysis) and MIC determination. The anti-*Mtb* drug ciprofloxacin is used a positive control.

The FAAL32 enzyme being involved in a key step of the mycolic acid biosynthesis pathway, the effect of closantel was investigated on closantel-treated Mtb cells following [1-^{14}C]acetate labelling and lipid extraction. The fatty acid (FA) and mycolic acid (MA) profiles were analyzed by thin-layer chromatography (Fig. S2) and showed that, in contrast to intact FA and MA profiles upon p-aminosalicylic acid treatment (targeting folic acid biosynthesis and used as negative control), cultures treated with closantel showed no residual lipids at 4x their respective MIC (Fig. S2A). Dose response investigation of the closantel effect indicates that both FAs and MAs are affected (Fig. S2B).

Binding of the salicylanilides closantel and rafoxanide to FAAL32 protein. Among the salicylanilides tested, in addition to closantel, rafoxanide displayed the highest inhibition rate both on FAAL32 activity and on Mtb viability (MIC 0.08 µM) (Fig. 3). We therefore decided to investigate the interaction of these compounds with the protein. The thermal stability of FAAL32 in the presence of these ligands was analyzed by monitoring its thermal unfolding under different concentrations of closantel and rafoxanide (Fig. 4A). As a positive control, we first investigated by nanoDSF the ability of AMPC12 to induce a shift in the melting temperature (T_m) of the protein. The addition of AMPC12 led to a significant thermal shift (ΔT_m). For instance, at 5 µM FAAL32 concentration and 50 µM of AMPC12, we obtained a ΔT_m value of 8.6 °C, which correlates with the already reported value (*6*) from T_m measurements using DSF in the presence of SyPro (ΔT_m value of 7.7 °C).

A clear shift of T_m towards higher values is visible in the fluorescence ratio plots for each of the 2 ligands compared with the free protein (Fig. 4A). Quantification of T_m under different ligand concentration shows a saturation at 5 and 2.5 µM for closantel and rafoxanide, respectively, suggesting a slightly improved affinity for rafoxanide. In both cases, ΔT_m values reach 2.7 °C. This confirms that closantel and rafoxanide are "binders" of FAAL32 and strongly suggests that the salicylanilide scaffold inhibits Mtb, at least partly, through inhibition of FAAL32 activity.

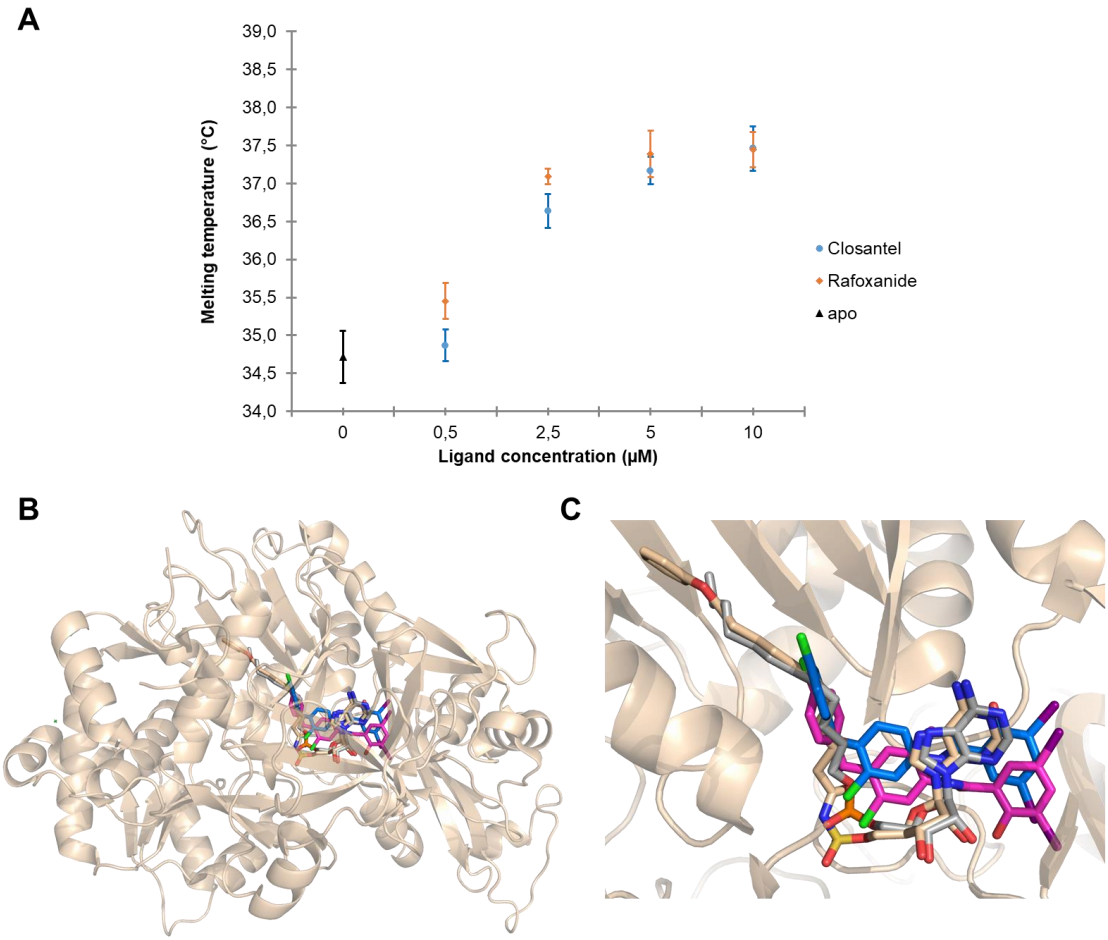

Fig. 4: **Binding of closantel and rafoxanide to FAAL32. A**. Assessment of FAAL32 protein thermal unfolding in presence of closantel and rafoxanide. For melting temperature (T_m) measurements, FAAL32 was mixed with DMSO (apo form, free protein) or with different amounts of closantel or rafoxanide (0.5 µM FAAL32 and 0.5-10 µM for ligand) and fluorescence was monitored at both 330 and 350 nm, using Prometheus Panta (NanoTemperTechnologies). **B.** Superposition of the overall structure of Mtb FAAL32 in complex with the 5'-O-[(11-phenoxyundecanoyl)sulfamoyl]adenosine inhibitor (wheat; pdb code 5HM3 [Kuhn *et al.,* 2016]), the AMPC12 molecule (gray) as observed in the structure of *M. marinum* FAAL32 complex (pdb code 5EY9 [Guillet *et al.,* 2016]) and the closantel (magenta) and the rafoxamide (ligth blue), as docked into the Mtb FAAL32 binding pocket. **C.** Close-up view of the binding pocket.

In order to further investigate their binding, docking of the salicylanilides on various conformations of the FAAL32 protein structure was performed. The five best poses, as identified by the lowest Vina score, were used to estimate the binding energy using the MM-PB/GBSA methods. Although this approach estimates the enthalpic term of the binding energy and does not take into account the entropic contribution, it nevertheless allows for comparison of compounds in a drug design

perspective (*33*). Rafoxanide and closantel display comparable binding energies (-49.6 and -49.2 kcal.mol^{-1}, respectively), much more favorable than oxyclozanide (-37.9 kcal.mol^{-1}) and nitazoxanide (-34.4 kcal.mol^{-1}). Closantel and rafoxanide display a similar binding mode and are predicted to bind at the nucleotide binding site of AMPC12 and 5'-O-[(11-phenoxyundecanoyl)sulfamoyl]adenosine (Fig. 4B-C).

Conclusions

In conclusion, here we report the optimization and automatization of a biochemical HTS for discovery of FAAL32 inhibitors. Using this assay, we screened a 1280-compound drug repurposing library. Primary and secondary screens led to the identification and validation of a salicylanilide pharmacophore-containing compound, closantel, which exhibited a MIC of 0.08 µM, better than the first-line antituberculous drug INH (MIC 0.6 µM (*19*)) or ciprofloxacin (MIC 1.25 µM, Fig. 3B). Altogether, our data confirm that hit selection based on inhibition of FAAL32, involved in an essential step of the cell envelope biosynthesis, is able to deliver molecules with anti-Mtb activity, and that salicylanilide represents a valuable antimycobacterial pharmacophore. Docking of the salicylanilides onto the FAAL32 protein structure provides insights into their binding mode and allowing for comparison of binding sites of FAAL32 inhibitors, in a drug design and development perspective.

ASSOCIATED CONTENT

Supplementary Table S1

Supplementary Table S2

Supplementary Figure S1

Supplementary Figure S2

AUTHOR INFORMATION

Corresponding Authors

* Hedia Marrakchi (hedia.marrakchi@ipbs.fr); Pierre Verhaeghe (pierre.verhaeghe@lcc-toulouse.fr); Lionel Mourey (lionel.mourey@ipbs.fr)

Author Contributions

The manuscript was written through contributions of all authors. All authors have given approval to the final version of the manuscript.

Funding Sources

The authors gratefully acknowledge financial support from the Agence Nationale de la Recherche (FASMY, grant ANR-14-CE16-0012) and the Région Midi-Pyrénées (MYCA, grants 34249 and 09005193).

ACKNOWLEDGMENT

We thank NanoTemper Technologies GmbH, in particular Pierre Soule and Cyril Castel, for their technical expertise and for making the microscale thermophoresis equipment available. We also thank Dr. Patrice Gouet for his precious help with ESPript software. We acknowledge the Integrated Screening Platform of Toulouse (PICT, IPBS, IBiSA) for the differential scanning fluorimetry and the macromolecular crystallography equipment used in this study.

ABBREVIATIONS

Mtb: *Mycobacterium tuberculosis*; FAAL: fatty acyl-AMP ligase; MA: mycolic acid; AMPC12: Adenosine 5′-dodecyl phosphate; MIC: minimum inhibitory concentration; IC_{50}: half-inhibitory concentration

REFERENCES

1. World Health Organization, Global Tuberculosis Report 2021. *Glob. Tuberc. Rep.*, 1–57 (2021).

2. J. C. Joanna, V. Mizrahi, *Priming the tuberculosis drug pipeline: new antimycobacterial targets and agents* (2018; https://pubmed.ncbi.nlm.nih.gov/29482115/), vol. 45.

3. A. Quémard, *New Insights into the Mycolate-Containing Compound Biosynthesis and Transport in Mycobacteria* (2016; https://pubmed.ncbi.nlm.nih.gov/27268593/), vol. 24.

4. M. Daffé, H. Marrakchi, Unraveling the Structure of the Mycobacterial Envelope. *Microbiol. Spectr.* **7** (2019), doi:10.1128/microbiolspec.gpp3-0027-2018.

5. H. Marrakchi, M. A. Lanéelle, M. Daffé, Mycolic Acids: Structures, Biosynthesis, and Beyond. *Chem. Biol.* **21**, 67–85 (2014).

6. V. Guillet, S. Galandrin, L. Maveyraud, S. Ladevèze, V. Mariaule, C. Bon, N. Eynard, M. Daffé, H. Marrakchi, L. Mourey, Insight into structure-function relationships and inhibition of the fatty Acyl-AMP ligase (FadD32) orthologs from mycobacteria. *J. Biol. Chem.* **291**, 7973–7989 (2016).

7. M. L. Kuhn, E. Alexander, G. Minasov, H. J. Page, Z. Warwrzak, L. Shuvalova, K. J. Flores, D. J. Wilson, C. Shi, C. C. Aldrich, W. F. Anderson, Structure of the Essential Mtb FadD32 Enzyme. *ACS Infect. Dis.* **2**, 579–591 (2016).

8. M. Léger, S. Gavalda, V. Guillet, B. van der Rest, N. Slama, H. Montrozier, L. Mourey, A. Quémard, M. Daffé, H. Marrakchi, The Dual Function of the Mycobacterium tuberculosis FadD32 Required for Mycolic Acid Biosynthesis. *Chem. Biol.* **16**, 510–519 (2009).

9. S. Gavalda, M. Léger, B. van der Rest, A. Stella, F. Bardou, H. Montrozier, C. Chalut, O. Burlet-Schiltz, H. Marrakchi, M. Daffé, A. Quémard, The Pks13/FadD32 crosstalk for the biosynthesis of mycolic acids in Mycobacterium tuberculosis. *J. Biol. Chem.* **284**, 19255–19264 (2009).

10. D. Portevin, C. De Sousa-D'Auria, H. Montrozier, C. Houssin, A. Stella, M. A. Lanéelle, F. Bardou, C. Guilhot, M. Daffé, The acyl-AMP ligase FadD32 and AccD4-containing acyl-CoA carboxylase are required for the synthesis of mycolic acids and essential for mycobacterial growth: Identification

of the carboxylation product and determination of the acyl-CoA carboxylase components. *J. Biol. Chem.* **280**, 8862–8874 (2005).

11. D. Portevin, C. De Sousa-D'Auria, C. Houssin, C. Grimaldi, M. Chami, M. Daffé, C. Guilhot, A polyketide synthase catalyzes the last condensation step of mycolic acid biosynthesis in mycobacteria and related organisms. *Proc. Natl. Acad. Sci. U. S. A.* **101**, 314–319 (2004).

12. F. Forti, A. Crosta, D. Ghisotti, Pristinamycin-inducible gene regulation in mycobacteria. *J. Biotechnol.* **140**, 270–277 (2009).

13. S. A. Stanley, T. Kawate, N. Iwase, M. Shimizu, A. E. Clatworthy, E. Kazyanskaya, J. C. Sacchettini, T. R. Ioerger, N. A. Siddiqi, S. Minami, J. A. Aquadro, S. S. Grant, E. J. Rubin, D. T. Hung, Diarylcoumarins inhibit mycolic acid biosynthesis and kill Mycobacterium tuberculosis by targeting FadD32. *Proc. Natl. Acad. Sci. U. S. A.* **110**, 11565–11570 (2013).

14. C. Fang, K. K. Lee, R. Nietupski, R. H. Bates, R. Fernandez-Menendez, E. M. Lopez-Roman, L. Guijarro-Lopez, Y. Yin, Z. Peng, J. E. Gomez, S. Fisher, D. Barros-Aguirre, B. K. Hubbard, M. H. Serrano-Wu, D. T. Hung, Discovery of heterocyclic replacements for the coumarin core of anti-tubercular FadD32 inhibitors. *Bioorg. Med. Chem. Lett.* **28**, 3529–3533 (2018).

15. M. Trawally, K. Demir-Yazıcı, S. İ. Dingiş-Birgül, K. Kaya, A. Akdemir, Ö. Güzel-Akdemir, Mandelic acid-based spirothiazolidinones targeting M. tuberculosis: Synthesis, in vitro and in silico investigations. *Bioorg. Chem.* **121**, 105688 (2022).

16. N. T. P. Ngidi, K. E. Machaba, N. N. Mhlongo, In Silico Drug Repurposing Approach: Investigation of Mycobacterium tuberculosis FadD32 Targeted by FDA-Approved Drugs. *Molecules*. **27** (2022), doi:10.3390/MOLECULES27030668.

17. S. Galandrin, V. Guillet, R. S. Rane, M. Léger, N. Radha, N. Eynard, K. Das, T. S. Balganesh, L. Mourey, M. Daffé, H. Marrakchi, Assay development for identifying inhibitors of the mycobacterial FadD32 activity. *J. Biomol. Screen.* **18**, 576–587 (2013).

18. N.-H. N. H. Le, V. Molle, N. Eynard, M. Miras, A. Stella, F. Bardou, S. Galandrin, V. Guillet, G. André-Leroux, M. Bellinzoni, P. Alzari, L. Mourey, O. Burlet-Schiltz, M. Daffé, H. Marrakchi, Ser/Thr phosphorylation regulates the fatty Acyl-AMP ligase activity of FadD32, an essential enzyme in mycolic acid biosynthesis. *J. Biol. Chem.* **291**, 22793–22805 (2016).

19. P. De, G. Koumba Yoya, P. Constant, F. Bedos-Belval, H. Duran, N. Saffon, M. Daffé, M. Baltas, Design, synthesis, and biological evaluation of new cinnamic derivatives as antituberculosis agents. *J. Med. Chem.* **54**, 1449–1461 (2011).

20. O. Trott, A. J. Olson, AutoDock Vina: Improving the speed and accuracy of docking with a new scoring function, efficient optimization, and multithreading. *J. Comput. Chem.* **31**, 455–461 (2010).

21. G. Menchon, L. Maveyraud, G. Czaplicki, Molecular dynamics as a tool for virtual ligand screening. *Methods Mol. Biol.* **1762**, 145–178 (2018).

22. R. Salomon-Ferrer, D. A. Case, R. C. Walker, An overview of the Amber biomolecular simulation package. *Wiley Interdiscip. Rev. Comput. Mol. Sci.* **3**, 198–210 (2013).

23. B. R. Miller, T. D. McGee, J. M. Swails, N. Homeyer, H. Gohlke, A. E. Roitberg, MMPBSA.py: An Efficient Program for End-State Free Energy Calculations. *J. Chem. Theory Comput.* **8**, 3314–3321 (2012).

24. K. Waisser, O. Bureš, P. Holý, J. Kuneš, R. Oswald, L. Jirásková, M. Pour, V. Klimešová, L. Kubicová, J. Kaustová, Relationship between the structure and antimycobacterial activity of substituted salicylanilides. *Arch. Pharm. (Weinheim).* **336**, 53–71 (2003).

25. G. Paraskevopoulos, S. Monteiro, R. Vosátka, M. Krátký, L. Navrátilová, F. Trejtnar, J. Stolaříková, J. Vinšová, Novel salicylanilides from 4,5-dihalogenated salicylic acids: Synthesis, antimicrobial activity and cytotoxicity. *Bioorganic Med. Chem.* **25**, 1524–1532 (2017).

26. M. Krátký, O. Janďourek, Z. Baranyai, E. Novotná, J. Stolaříková, S. Bősze, J. Vinšová, Phenolic N-monosubstituted carbamates: Antitubercular and toxicity evaluation of multi-targeting

compounds. *Eur. J. Med. Chem.* **181** (2019), doi:10.1016/j.ejmech.2019.111578.

27. X. Z. Fan, J. Xu, M. Files, J. D. Cirillo, J. J. Endsley, J. Zhou, M. A. Endsley, Dual activity of niclosamide to suppress replication of integrated HIV-1 and Mycobacterium tuberculosis (Beijing). *Tuberculosis.* **116**, S28–S33 (2019).

28. M. Krátký, J. Vinšová, E. Novotná, J. Stolaříková, Salicylanilide pyrazinoates inhibit in vitro multidrug-resistant Mycobacterium tuberculosis strains, atypical mycobacteria and isocitrate lyase. *Eur. J. Pharm. Sci.* **53**, 1–9 (2014).

29. I. Y. Lee, T. D. Gruber, A. Samuels, M. Yun, B. Nam, M. Kang, K. Crowley, B. Winterroth, H. I. Boshoff, C. E. Barry, Structure-activity relationships of antitubercular salicylanilides consistent with disruption of the proton gradient via proton shuttling. *Bioorganic Med. Chem.* **21**, 114–126 (2013).

30. M. Krátký, J. Vinová, E. Novotná, J. Mandíková, V. Wsól, F. Trejtnar, V. Ulmann, J. Stolaíková, S. Fernandes, S. Bhat, J. O. Liu, Salicylanilide derivatives block Mycobacterium tuberculosis through inhibition of isocitrate lyase and methionine aminopeptidase. *Tuberculosis.* **92**, 434–439 (2012).

31. M. Gooyit, K. D. Janda, Reprofiled anthelmintics abate hypervirulent stationary-phase Clostridium difficile. *Sci. Rep.* **6**, 1–8 (2016).

32. S. Ghods, E. K. Pour, H. Riazi-Esfahani, H. Faghihi, B. Inanloo, Closantel Retinal Toxicity: Case Report and Literature Review. *Case Rep. Ophthalmol. Med.* **2021**, 1–4 (2021).

33. E. Wang, H. Sun, J. Wang, Z. Wang, H. Liu, J. Z. H. Zhang, T. Hou, End-Point Binding Free Energy Calculation with MM/PBSA and MM/GBSA: Strategies and Applications in Drug Design. *Chem. Rev.* **119**, 9478–9508 (2019).